Comment on "Cleavage surface of the $BaFe_{2-x}Co_xAs_2$ and $Fe_ySe_{1-x}Te_x$ superconductors: A combined STM plus LEED study"

M. Cordin, P. Amann,* A. Menzel, and E. Bertel
Institute of Physical Chemistry, University of Innsbruck, Innrain 52a, 6020 Innsbruck, Austria

M. Baranov and S. Diehl
Institute of Theoretical Physics, University of Innsbruck and Institute for Quantum Optics and Quantum Information, Austrian Academy of Sciences, Otto-Hittmair-Platz 1, 6020 Innsbruck, Austria

J. Redinger
Institute of Applied Physics, Vienna University of Technology, Gusshausstrasse 25/134, 1040 Vienna, Austria

C. Franchini
Faculty of Physics, University of Vienna, Strudlhofgasse 4, 1090 Vienna, Austria

(Received 26 April 2012; revised manuscript received 3 September 2012; published 19 October 2012)

Massee *et al*. [Phys. Rev. B **80**, 140507(R) (2009)] found on the cleavage planes of $BaFe_{2-x}Co_xAs_2$ two different long-range ordered structures, i.e., a (2×1) phase present only after cleavage at low temperature and a $\sqrt{2} \times \sqrt{2}$ phase observed after cleavage at room temperature. These results apply generally to 122 Fe-based superconductors, but have been discussed controversially [for a summary of the conflicting views, see Hoffman, Rep. Prog. Phys. **74**, 124513 (2011)]. Here we support the interpretation of Massee *et al*. In addition, we argue that the existence of different long-range ordered structures corresponding to the same coverage in different temperature regimes is associated with the melting of a charge density wave and removal of an associated periodic lattice distortion (CDW/PLD) in the substrate as T is increased. At sufficiently low temperature the fluctuating CDW/PLD order parameter is stabilized by the adsorbate in a lock-in type mechanism. Accordingly, we interpret the surface structures observed on the 122 Fe pnictide surfaces as evidence for the presence of CDW fluctuations at low temperature, but *with a wave vector differing from that of the antiferromagnetic spin-density fluctuations*.

DOI: 10.1103/PhysRevB.86.167401 PACS number(s): 68.65.−k, 68.35.Rh, 75.25.Dk, 74.70.Xa

Recently, a debate arose about the surface termination of cleaved 122 Fe-based superconductor samples deriving from parent compounds with stoichiometry AFe_2As_2, where A is an alkaline earth metal (Ca, Sr, or Ba). The scanning tunneling microscopy (STM) data reveal a multitude of different ordered and disordered structures depending on the precise cleaving conditions.[1] These structures have been interpreted in essentially two different ways: Either they are attributed to a half-monolayer (0.5 ML) of alkaline earth metals (Ca, Sr, or Ba)[1–5] or they are thought to arise from a reconstruction of the As layer.[6–8] In the first case the surface would be nonpolar; in the latter case it would be polar, which of course has some significance for the interpretation of the spectroscopic data. The pros and cons for each interpretation are succinctly summarized in Ref. 9. Here we discuss the observations from a surface science point of view. By showing similar data from an entirely different surface system we argue in favor of an adsorbate layer, i.e., a nonpolar surface in agreement with Massee *et al*.[1] The observation of two different long-range ordered structures is interpreted in terms of an order-order phase transition, which is driven by the substrate. Specifically, it is attributed to the competition between a fluctuating charge density wave (CDW) order parameter (OP) and the adsorbate-adsorbate repulsion (AAR). Using an extended Landau theory for the phase transition we propose that at sufficiently low temperature the CDW-OP is stabilized by the adsorbate layer in a kind of bootstrap mechanism. At room temperature, in contrast, the surface structure is dictated by the AAR. The disordered structures result from kinetic barriers in the surface system. This interpretation suggests the existence of CDW-OP fluctuations and a concomitant fluctuating periodic lattice distortion in the substrate, respectively, the As-Fe_2-As layer. Notably, however, *the direction of the CDW wave vector differs from the spin-density wave vector*.

In essence, the structures observed upon cleaving of 122 FeAs compounds can be grouped into three classes: (i) a long-range ordered (2×1) structure found after cleaving at low temperature ($T \sim 10$ K); (ii) a long-range ordered $\sqrt{2} \times \sqrt{2}$ structure typically found after cleaving at $T > 200$ K; and (iii) various disordered structures consisting either of mixed structural elements from (i) and (ii), completely disordered areas, or linear defect structures (domain boundaries, rodlike structures). The low-T (2×1) structure is irreversibly destroyed upon heating.

Structure models for (i) and (ii) based on the assumption that the structures arise from a 0.5 ML alkaline earth metal coverage are displayed in Figs. 1(a) and 1(b). Note that the $\sqrt{2} \times \sqrt{2}$ unit cell is rotated 45° with respect to the substrate surface unit cell. An alternative notation is to use an unrotated nonprimitive centered unit cell $c(2 \times 2)$. Below, we will call this the checkerboard structure, while the (2×1) structure will be designated as the rectangular structure. An analogous phase transition is found in the adsorbate system Br/Pt(110), which sheds some light on the mechanism.

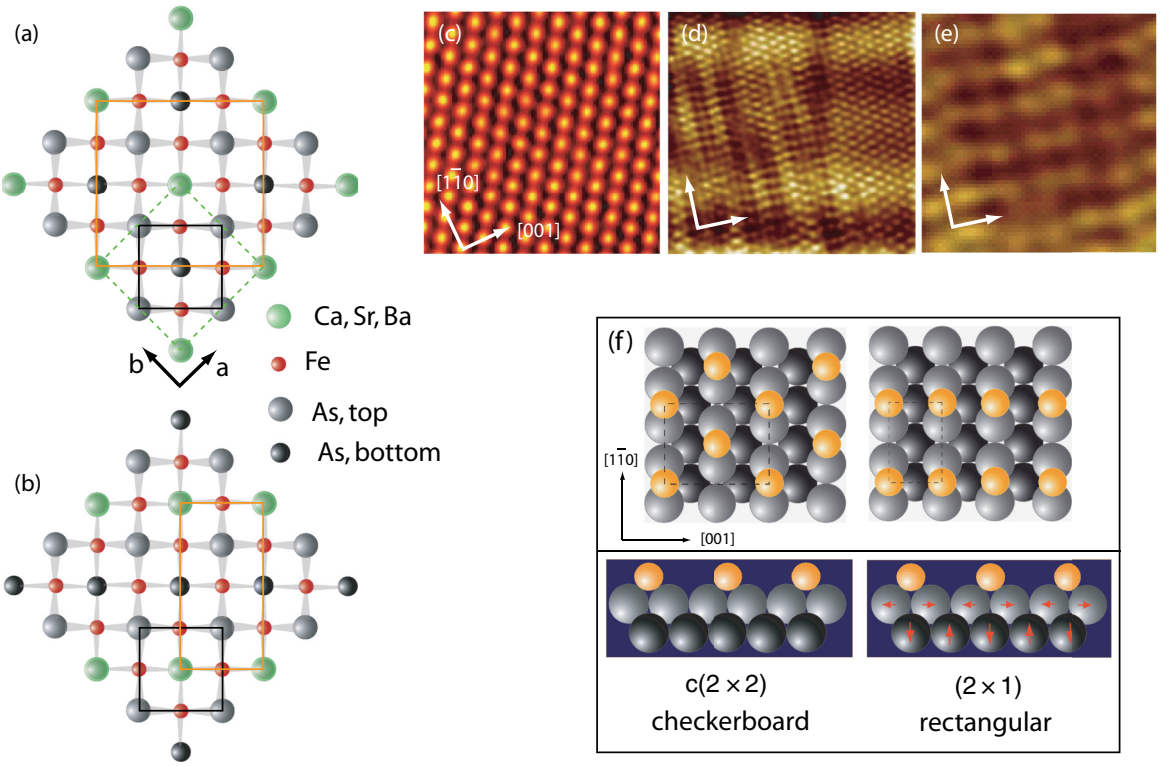

FIG. 1. (Color) (a) Structural model for the AFe_2As_2 (A: alkaline earth metal) cleavage surface with $\sqrt{2} \times \sqrt{2}$ structure assuming the latter to be formed by adatoms; black square: (1 × 1) surface unit cell; dashed green square: $\sqrt{2} \times \sqrt{2}$ unit cell; orange square: $c(2 \times 2)$ unit cell. (b) Same cleavage surface with (2 × 1) structure; orange rectangle: (2 × 1) unit cell. (c) $c(2 \times 2)$ structure of Br on Pt(110) imaged at room temperature. (d) Coexistence of $c(2 \times 2)$ and (2 × 1) Br structures on Pt(110) at 50 K. (e) Zoom-in from (d) showing (2 × 1) rectangular structure. Note that the two structures fluctuate at 50 K slowly transforming into each other. (f) Structural models for the two structures shown in (c)–(e).

I. BRIEF ACCOUNT OF THE ($\sqrt{2} \times \sqrt{2}$) ↔ (2 × 1) PHASE TRANSITION IN Br/Pt(110)

Figuress 1(c)–1(f) show structures found in the surface system Br/Pt(110). The checkerboard structure is perfectly ordered at room temperature, while the rectangular structure appears only at cryogenic temperatures. According to density-functional theory (DFT) calculations,[10] the rectangular structure is the ground state at 0 K. To find two long-range ordered structures corresponding to the same coverage but prevailing in different temperature regimes is an extremely rare case for surface systems and has been attributed to significantly higher vibrational entropy of the adsorbate in the new bonding sites of the high-T phase.[11] This explanation fails in the present case, since the local bonding site is the same in the rectangular and checkerboard phase, respectively. Hence the phase transition cannot be rationalized by considering the adsorbate layer alone. As previously discussed[10] (see also the Supplemental Material[12]) the substrate exhibits a periodic lattice distortion (PLD) and a concomitant charge density modulation, i.e., a CDW in the rectangular structure, which is absent in the checkerboard phase. The energy costs for straining the substrate and for the higher AAR in the rectangular phase are apparently compensated by the more favorable binding sites offered to the adsorbate on the periodically modulated substrate. As the temperature is raised, an increase in both electronic and lattice entropy lead to the destruction of the CDW/PLD in the substrate. The adsorbate then rearranges into the checkerboard phase thereby minimizing the AAR. The latter phase disappears at a substantially higher T_c in a continuous order-disorder transition.[13] Due to the anisotropy of the Pt(110) surface, the rectangular-to-checkerboard transition can be cast into a one-dimensional model in the spirit of the Landau theory for phase transitions:[10]

$$F = J \sum_j s_j s_{j+1} + gm \sum_j s_j + \frac{L}{a}\left(\frac{\alpha_0}{2}\left(T - T_c^P\right)m^2 + \frac{\lambda}{4}m^4\right). \quad (1)$$

Here F is the one-dimensional (1D) free-energy density, L is the sample dimension, a is the row-to-row distance, J is the nearest-neighbor repulsion, and $s_j = \pm 1/2$ is an occupation number assigned to a lattice site j, depending on whether it is occupied or not. m is the CDW/PLD-OP and T_c^P is the critical temperature for the PLD/CDW transition of the pure substrate. It corresponds to the disordering temperature of the PLD/CDW phase of a clean surface. T_c^P might even be negative, meaning that the CDW order parameter is zero for all temperatures on the clean substrate.

The first term in Eq. (1) represents the AAR and favors the checkerboard structure. The second term represents the coupling of the adsorbate to the PLD/CDW in the substrate:

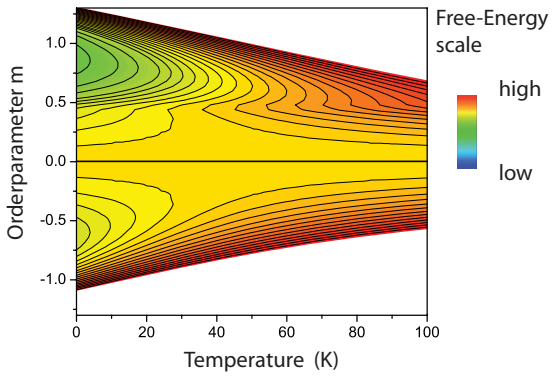

FIG. 2. (Color) A model free-energy surface based on Eq. (1). The upper half shows the free-energy surface with a coupling parameter $g < 0$. For the free-energy surface shown in the lower half, g has been set to zero. The free energy varies from low (green) to high (red). Note the stabilization of a finite order parameter to higher temperatures and the presence of a barrier between two degenerate states with $m = 0$ and $m = 0.7$, which is characteristic of a (weakly) first-order transition.

Assuming without loss of generality $g < 0$, one obtains an energy gain in the rectangular structure from locking the adsorbate atoms onto the CDW maxima. If this coupling term is large enough, it stabilizes a finite order parameter m by overcompensating for the repulsive energy in the adlayer. This renders the rectangular structure the preferred ground state. Figure 2 shows a model calculation of the free-energy surface using the minimal model from Eq. (1). In the lower half of the diagram the free-energy surface is shown for $g = 0$ and $T_c^P = 40$ K. In this case the lattice distortion (m finite) persists only at very low temperatures. The adsorbate invariably adopts a quasihexagonal packing up to the disordering T_c. The upper half of the diagram applies, if $g < 0$. The coupling term has the effect of an external field. It stabilizes a finite OP up to much higher temperatures, and at sufficiently low T the adsorbate is forced into the rectangular (2×1) structure. The transition to a flat substrate ($m = 0$) and the $c(2 \times 2)$ checkerboard phase of the adsorbate is weakly first order as required by Landau theory for order-order transitions.

II. $(\sqrt{2} \times \sqrt{2}) \leftrightarrow (2 \times 1)$ PHASE TRANSITION IN $A\mathrm{Fe_2As_2}$

The above discussion of the rectangular $\rightarrow$ checkerboard transition can be transferred almost one to one to the case of the 122 Fe pnictides, if it is assumed that the structures arise from a half-layer of adatoms. This assumption is supported by DFT calculations of Gao *et al.*[14] These authors found the cleavage surfaces with $c(2 \times 2)$ or (2×1) A adatom superstructure to be considerably more stable than a pair of cleavage surfaces with As and (1×1) A adatom termination, respectively. Similar to the Br/Pt(110) system the $c(2 \times 2)$ structure is associated with a flat, and the (2×1) with a buckled FeAs layer. This result is qualitatively confirmed in a low-energy electron diffraction (LEED) analysis of $\mathrm{BaFe_{2-x}Co_xAs_2}$ by van Heumen *et al.*[15] However, DFT calculations refer to the ground state ($T = 0$ K) and therefore are not able to explain why the long-range ordered (2×1) structure is preferred at low temperature, while

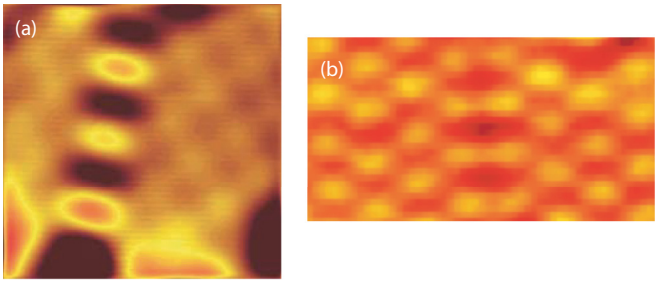

FIG. 3. (Color) (a) Checkerboard and rectangular structure coexisting on $\mathrm{SrFe_2As_2}$ [Niestemski *et al.* (Ref. 8)] (reprinted with kind permission by the authors); (b) checkerboard and rectangular structure coexisting on Br/Pt(110) at 50 K.

the $c(2 \times 2)$ structure prevails at room temperature. As in the halogen/Pt(110) system, the free energy of the adlayer alone cannot account for this phenomenon. The local bonding site of the A atoms involving a fourfold coordination to the As atoms is the same for both rectangular and checkerboard structures. Thus, the relative stability of the two structures has to involve the substrate As-$\mathrm{Fe_2}$-As layer. At low T the coupling to a CDW/PLD stabilizes the (2×1) structure, while at high T the CDW/PLD is destroyed and interadsorbate repulsion favors the $c(2 \times 2)$ structure, just as for Br on Pt(110). Figure 3 illustrates the similarity of the two surface systems. It shows the coexistence of the checkerboard phase with a stripe of the rectangular phase on $\mathrm{SrFe_2As_2}$ [Fig. 3(a)][8] and on Br/Pt(110) [Fig. 3(b)].

Interestingly, the DFT calculations by Gao *et al.*[14] indicate a clear trend in the relative stability of checkerboard versus rectangular structure with the former being the most stable for Ba, not so much preferred for Sr, and less stable than the rectangular structure for Ca. Equation (1) provides a simple and almost intuitive explanation for this trend: The relative stability depends on the balance between the energy gain provided by the coupling g to the CDW and the repulsive energy cost J. The latter is expected to decrease along the sequence Ba, Sr, Ca, so that for Ca only the rectangular structure is observed. This is again a close analogy to the halogen/Pt(110) system, where for the smaller Cl the rectangular structure is stable up to room temperature (see also the schematic phase diagram Fig. 2 and the associated discussion in Ref. 10). Gao *et al.* predicted the ground state for Ba to be the $c(2 \times 2)$ structure in contrast to the experimental observations.[1] Presumably this can be attributed to strong correlation effects in the Fe pnictides increasing the error margins of absolute DFT values, while the relative trends should be captured quite well.

Clearly, there are differences between the two surface systems. The substrate unit cell is rectangular on Pt(110) as opposed to the square unit cell of the (undistorted) As-$\mathrm{Fe_2}$-As layer. As a consequence, two rotational domains of the (2×1) structure are present in the latter case.[16] In principle, the 1D model of Eq. (1) has to be replaced by a two-dimensional (2D) version, since here interactions are equivalent in the two orthogonal directions. However, with the first term in Eq. (1) representing the AAR, its effect is the same in both the 1D and the 2D models, namely, a preference for the checkerboard

structure. The other two terms in Eq. (1) are zero if $m = 0$. $m \neq 0$ requires a spontaneous breaking of the fourfold symmetry. This is consistent with the recently observed nematicity of 122 superconductors.[16,17] Thus the use of a 1D model is justified to some extent in the presence of CDW fluctuations. Of course, this simplified version should not be applied for extracting quantitative information, but it serves well to illustrate the basic mechanism.

A further difference is the reversibility of the phase transition in the case of Br/Pt(110), while it is irreversible for the 122 FeAs compounds. There are two different mechanisms which can contribute to the irreversibility. First, the transition is first order. Therefore there is a barrier between the two phases as also illustrated in the upper half of Fig. 2. For Br/Pt(110) this barrier is so small as to allow fluctuations between the two phases at 50 K. However, the fluctuations are sufficiently slow to be imaged by STM in the constant current mode (typical time scale: several seconds). With a significantly larger barrier a conversion between the phases is kinetically hindered. This would give rise to a hysteresis, but one should still find the system in either of the two long-range ordered phases. However, in addition to the barrier in the free-energy surface a checkerboard-to-rectangular conversion is hampered by an atomic diffusion barrier, because it requires a site change of the A atoms. The observation of disordered structures under most cleaving conditions suggests that this diffusion barrier is rather high, preventing a postcleavage ordering. The long-range ordered rectangular structure could then only be established in the cleavage process itself, because this does not require a site change. Note that this explanation suggests the *disordered* structures to be metastable at low temperature. The present view differs from the interpretation of Hoffman,[9] who proposed the *rectangular* structure to be metastable. The strong kinetic barriers obviously present in the system support the assignment of the structures to adatoms rather than a reconstruction of the As layer.

The low-T rectangular structure of Br/Pt(110) is attributable to CDW-OP fluctuations on the Pt surface[18] which are stabilized in a lock-in type mechanism by the adsorbate.[10,19] The strong Kohn anomaly found in bulk Pt (Ref. 20) supports this assignment. For the rectangular phase on $SrFe_2As_2$, Niestemski *et al.* dismissed a CDW order as possible origin, because there is no appropriate Fermi-surface nesting vector and there is no contrast reversal in STM imaging as the STM bias is inverted. The latter argument is void, if the CDW is decorated by an adsorbate as postulated here. The absence of an appropriate Fermi-surface nesting needs to be considered in detail. The wave vector $\mathbf{q}_{2\times1} = (\pm\pi/2, \pm\pi/2)$ [unfolded surface Brillouin zone (SBZ)] characterizing the rectangular structure is 45° rotated from the nesting vector $\mathbf{q}_{\mathrm{AF}} = (0, \pm\pi)$ or $(\pm\pi, 0)$ responsible for the antiferromagnetic order in the undoped parent compounds of the Fe-based superconductors. However, depending on doping and band renormalization, nesting vectors which span approximately half of the SBZ appear between opposite boundaries of the central hole pocket or of the electron pockets at the SBZ boundary (e.g., Fig. 4 in Ref. 21 or Fig. 9 in Ref. 22). In fact, a more complex topology of the Fermi surface around the X/Y point has been postulated in recent experimental studies, which

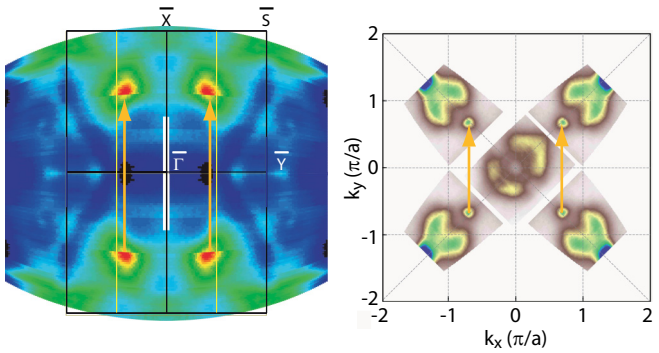

FIG. 4. (Color) (a) Fermi-surface mapping of Pt(110) (Ref. 19). Orange arrows mark the connecting wave vector between points of high density of state at E_F. (b) Fermi-surface mapping of $(Sr,K)Fe_2As_2$. (From Ref. 22, with permission, © 2010 Wiley-VCH.)

requires a careful reconsideration of nesting arguments.[23–25] Furthermore, the instability towards charge ordering arises from a maximum in the charge response function $\chi(\mathbf{q})$. For such a maximum to occur, extended Fermi-surface nesting is not necessarily required. As pointed out by Rice and Scott,[26] singular points at E_F, in particular, saddle points in a two-dimensional band structure, may be sufficient to trigger a CDW (see also the discussion of quasiparticle interference by Hoffman[9]). In Fig. 4 we compare a Fermi-surface mapping of the Pt(110) surface[19] with a Fermi-surface mapping of $(Sr,K)Fe_2As_2$,[22] both recorded with He I angle-resolved photoemission. The mapping shows points with very high density of states at E_F. It is true that in both cases the connecting vectors are larger than $\mathbf{q}_{2\times1}$. Actually, the resulting CDW would be incommensurate. Consequently, a static CDW phase is not stable. However, with 0.5 ML of an adsorbate being present, the coupling term in Eq. (1) provides sufficient stabilization energy to coax the fluctuating incommensurate into a static commensurate CDW/PLD phase. One should also be aware that nesting arguments have only limited predictive power, since the electronic energy contributions to the stabilization of a CDW-OP do not solely arise at the Fermi surface and in addition have to be weighted by the q-dependent electron-phonon coupling as discussed in detail by Johannes and Mazin.[27]

The preceding discussion bears some implications relevant for the study of superconductivity in Fe pnictides. First, the presence of CDW-OP fluctuations at low temperature is indicated. This is not new,[28,29] but the present interpretation suggests that the CDW wave vector is rotated by 45° with respect to the wave vector of the AF-OP. Of course this sheds no light on whether the CDW-OP fluctuations are accidental or whether they do take part in the pairing mechanism. Another consequence concerns the data evaluation. For instance, on every surface with the ordered rectangular structure a gap was detected by scanning tunneling spectroscopy. If the rectangular structure is attributed to a static CDW/PLD locked by the adsorbate, the gap could also be interpreted as a Peierls gap. For the electron-doped pnictide $BaCo_xFe_{2-x}As_2$ it has been shown that the gap is suppressed in vortex cores[3] and closes at the bulk T_c.[30] This is strong evidence for a superconducting rather than a Peierls gap. On the other

hand, the hole-doped $Ba_{0.6}K_{0.4}Fe_2As_2$ shows coexistence of different types of gaps.[31] Finally we remark that by virtue of the fluctuation-dissipation theorem, the presence of charge density fluctuations would imply a strongly enhanced charge response function, and therefore high polarizability and enhanced screening, which might be helpful for the Cooper pair bonding.[32–34]

ACKNOWLEDGMENTS

This work was supported by the Austrian Science Fund and by the University of Innsbruck through the research platform "Advanced Materials." We thank V. Madhavan and X. Zhou for permission to reproduce Figs. 3(a) and 4(b), respectively. E.B. gratefully acknowledges enlightening discussions with M. Golden.

---

*Present address: Vorarlberg University of Applied Sciences, Hochschulstrasse 1, 6850 Dornbirn, Austria.

[1] F. Massee, S. de Jong, Y. Huang, J. Kaas, E. van Heumen, J. B. Goedkoop, and M. S. Golden, Phys. Rev. B **80**, 140507 (2009).

[2] M. C. Boyer, K. Chatterjee, W. D. Wise, G. F. Chen, J. L. Luo, N. L. Wang, and E. W. Hudson, arXiv:0806.4400.

[3] Y. Yin, M. Zech, T. L. Williams, X. F. Wang, G. Wu, X. H. Chen, and J. E. Hoffman, Phys. Rev. Lett. **102**, 097002 (2009).

[4] D. Hsieh, Y. Xia, L. Wray, D. Qian, K. K. Gomes, A. Yazdani, G. F. Chen, J. L. Luo, N. L. Wang, and M. Z. Hasan, arXiv:0812.2289.

[5] H. Zhang *et al.*, Phys. Rev. B **81**, 104520 (2010).

[6] V. B. Nascimento *et al.*, Phys. Rev. Lett. **103**, 076104 (2009).

[7] G. Li *et al.*, arXiv:1006.5907.

[8] F. C. Niestemski, V. B. Nascimento, B. Hu, E. W. Plummer, J. Gillett, S. Sebastian, Z. Wang, and V. Madhavan, arXiv:0906.2761.

[9] J. E. Hoffman, Rep. Prog. Phys. **74**, 124513 (2011).

[10] M. Cordin, B. A. J. Lechner, P. Amann, A. Menzel, E. Bertel, C. Franchini, R. Zucca, J. Redinger, M. Baranov, and S. Diehl, Europhys. Lett. **92**, 26004 (2010).

[11] J. Gu, W. S. Sim, and D. A. King, J. Chem. Phys. **107**, 5613 (1997).

[12] See Supplemental Material at http://link.aps.org/supplemental/10.1103/PhysRevB.86.167401 for computational method and geometry parameters of the (2 × 1)-Br/Pt(110) surface.

[13] E. Doná *et al.*, Phys. Rev. Lett. **98**, 186101 (2007).

[14] M. Gao, F. Ma, Z.-Y. Lu, and T. Xiang, Phys. Rev. B **81**, 193409 (2010).

[15] E. van Heumen *et al.*, Phys. Rev. Lett. **106**, 027002 (2011).

[16] T.-M. Chuang, M. P. Allan, J. Lee, Y. Xie, N. Ni, S. L. Bud'ko, G. S. Boebinger, P. C. Canfield, and J. C. Davis, Science **327**, 181 (2010).

[17] J.-H. Chu, H.-H. Kuo, J. G. Analytis, and I. R. Fisher, Science **337**, 710 (2012).

[18] C. Deisl, K. Swamy, N. Memmel, E. Bertel, C. Franchini, G. Schneider, J. Redinger, S. Walter, L. Hammer, and K. Heinz, Phys. Rev. B **69**, 195405 (2004).

[19] P. Amann *et al.*, Eur. Phys. J. B **75**, 15 (2010).

[20] D. H. Dutton, B. N. Brockhouse, and A. P. Miiller, Can. J. Phys. **50**, 2915 (1972).

[21] S.-L. Yu, J. Kang, and J.-X. Li, Phys. Rev. B **79**, 064517 (2009).

[22] X. Zhou, G. Liu, J. Meng, W. Zhang, H. Liu, L. Zhao, and X. Jia, Phys. Status Solidi A **207**, 2674 (2010).

[23] T. Kondo *et al.*, Phys. Rev. B **81**, 060507 (2010).

[24] S. de Jong *et al.*, Europhys. Lett. **89**, 27007 (2010).

[25] V. B. Zabolotnyy *et al.*, Physica C **469**, 448 (2009).

[26] T. M. Rice and G. K. Scott, Phys. Rev. Lett. **35**, 120 (1975).

[27] M. D. Johannes and I. I. Mazin, Phys. Rev. B **77**, 165135 (2008).

[28] F. Wang and D.-H. Lee, Science **332**, 200 (2011).

[29] H. Zhai, F. Wang, and D.-H. Lee, Phys. Rev. B **80**, 064517 (2009).

[30] F. Massee, Y. K. Huang, J. Kaas, E. van Heumen, S. de Jong, R. Huisman, H. Luigjes, J. B. Goedkoop, and M. S. Golden, Europhys. Lett. **92**, 57012 (2010).

[31] D. H. Torchinsky, G. F. Chen, J. L. Luo, N. L. Wang, and N. Gedik, Phys. Rev. Lett. **105**, 027005 (2010).

[32] G. A. Sawatzky, I. S. Elfimov, J. van den Brink, and J. Zaanen, Europhys. Lett. **86**, 17006 (2009).

[33] M. Berciu, I. Elfimov, and G. A. Sawatzky, Phys. Rev. B **79**, 214507 (2009).

[34] R. Chan, M. Gulacsi, A. Ormeci, and A. R. Bishop, Phys. Rev. B **82**, 132503 (2010).